

MRI evaluation of the relationship between R_2 , R_2^* , and tissue iron in the human basal ganglia

Joanna Collingwood^{1,2}, Mary Finnegan¹, Zobair Arya³, Jean-Pierre Hagen¹, Saherabanu Chen¹, Alimul Chowdhury⁴, Sarah Wayte⁵, Eddie Ngandwe⁵, Naomi Visanji⁶, Jon Dobson⁷, Penny Gowland⁸, Lili-Naz Hazrati⁹, and Charles Hutchinson^{5,10}

¹School of Engineering, University of Warwick, Coventry, West Midlands, United Kingdom, ²Materials Science and Engineering, University of Florida, Gainesville, Florida, United States, ³Department of Physics, University of Warwick, West Midlands, United Kingdom, ⁴School of Psychology, University of Birmingham, West Midlands, United Kingdom, ⁵University Hospitals Coventry and Warwickshire, West Midlands, United Kingdom, ⁶Morton and Gloria Shulman Movement Disorders Centre, Toronto Western Hospital, Ontario, Canada, ⁷J. Crayton Pruitt Family Department of Biomedical Engineering, University of Florida, Florida, United States, ⁸School of Physics & Astronomy, University of Nottingham, Nottinghamshire, United Kingdom, ⁹Tanz Centre for Research in Neurodegenerative Disease, University of Toronto, Ontario, Canada, ¹⁰Warwick Medical School, University of Warwick, West Midlands, United Kingdom

Introduction: The use of structural MRI to assess brain iron has particular relevance if it can detect the iron changes that occur as a consequence of neurodegenerative disorders. At present, MRI techniques to measure tissue iron are better established for liver than for brain. One particular challenge for brain iron analysis is validation. MRI measurement of liver iron is directly validated with tissue iron content¹. For human brain, validation of the relationship between MRI parameters and iron is highly dependent on prior post-mortem analyses. The heterogeneity of the human brain, and the structural and chemical changes associated with neurodegenerative processes, lead to multiple sources of signal variation besides iron. It is therefore important to understand the factors affecting the measurement, and to find methods to validate the relationship between iron and relevant MRI parameters.

Methods: Post-mortem fresh-frozen tissues were dissected to obtain blocks of substantia nigra (SN), globus pallidus (GP), putamen (Pu), and caudate nucleus (CN) from two healthy cases. Proton relaxation rate (R_2) and R_2^* mapping of the blocks was performed at 9.4 T at 2 °C using a Bruker MicWB40 probe. Subsequently, the blocks were cryosectioned in the imaging plane, to enable determination of spatial iron distribution using synchrotron X-ray fluorescence (SXRF) mapping with 60 µm in-plane resolution. To explore options for clinical determination of R_2 and R_2^* , measurement of R_2 by various methods was performed at 1.5 T (Optima 360, GE) and 3.0 T (HDx, GE, and Achieva, Philips), and measurement of R_2^* performed at 3.0 T (Achieva, Philips), for a group of 10 healthy male volunteers aged between 20 and 70 years old.

Results: In the 9.4 T post-mortem study, a clear linear dependence of R_2 [Fig. 1] and R_2^* on iron concentration was observed for the SN, GP, Pu, and CN tissues that were analyzed, in grey and white matter regions:

$$R_2 = (0.072 \times [\text{Fe}]) + 20 \quad [\text{Eq. 1}]$$

$$R_2^* = (0.340 \times [\text{Fe}]) + 37 \quad [\text{Eq. 2}]$$

(Fe is in µg / g of prior frozen unfixed tissue, and R_2 , R_2^* are in s⁻¹.)

In the clinical measurements of R_2 and R_2^* at 3.0 T and 1.5 T, the computed R_2 values were significantly shorter when four single echo spin echo measurements (with $T_E = 10, 27.5, 45$, and 80 ms, $T_R = 2500$ ms) were used instead of multi-spin multi-echo sequences to obtain R_2 . The R_2 maps obtained at 1.5 T and 3.0 T were used to compute the field dependent R_2 increase (FDRI)², and were segmented in the axial plane to determine the average R_2 and FDRI values throughout regions of the basal ganglia including SN, Pu, and GP [Fig. 2].

Discussion: The post-mortem data provide direct evidence that the linear relationship between R_2 , R_2^* and iron is preserved at a field of 9.4 T, and the result for R_2 is consistent with the empirically obtained field-dependent relationship determined by Vymazal et al³. The preliminary clinical data support prior conclusions that single echo approaches give more consistent values than standard multi spin multi echo sequences¹. The relationship between iron and R_2 , R_2^* , shown here to hold at 9.4 T for the iron-rich regions in the basal ganglia, has scope to be utilized in identifying brain iron accumulation in disease, especially given the recent observation that Parkinson's disease, Multiple System Atrophy, and healthy controls may be differentiated post-mortem based on patterns of brain iron dysregulation and accumulation⁴.

References:

1. St Pierre T.G., et al, Noninvasive measurement and imaging of liver iron concentrations using proton magnetic resonance, *Blood* (2005) 105 p.855-861
2. Bartzokis G., et al, In vivo MR evaluation of age-related increases in brain iron, *AJNR* (1994) 15 p.1129-1138
3. Vymazal, J., et al., The relation between brain iron and NMR relaxation times: An in vitro study, *MRM* (1996) 35 p.56-61
4. Visanji N.P., et al, Iron Deficiency in Parkinsonism: Region-Specific Iron Dysregulation in Parkinson's Disease and Multiple System Atrophy, *Journal of Parkinson's Disease* (2013) in press (DOI 10.3233/JPD-130197)

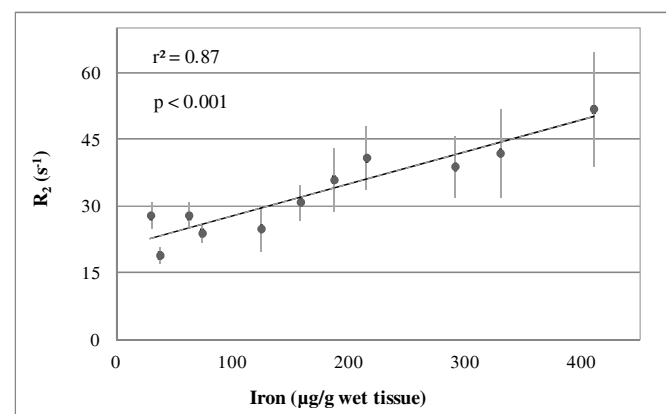


Figure 1: R_2 versus tissue iron concentration for regions in the basal ganglia (from two healthy cases, post mortem). Values are obtained by directly matching R_2 maps with iron maps obtained by SXRF.

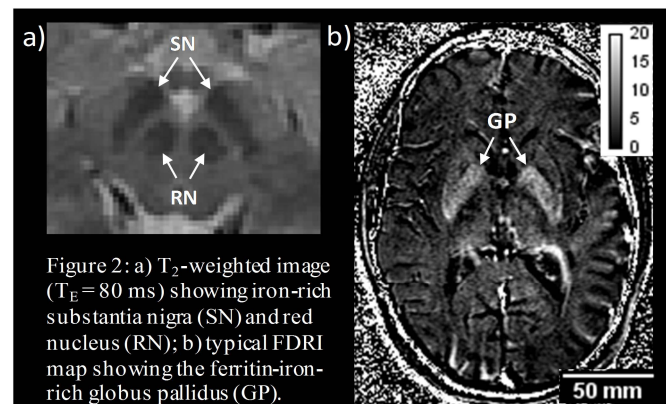


Figure 2: a) T_2 -weighted image ($T_E = 80$ ms) showing iron-rich substantia nigra (SN) and red nucleus (RN); b) typical FDRI map showing the ferritin-iron-rich globus pallidus (GP).